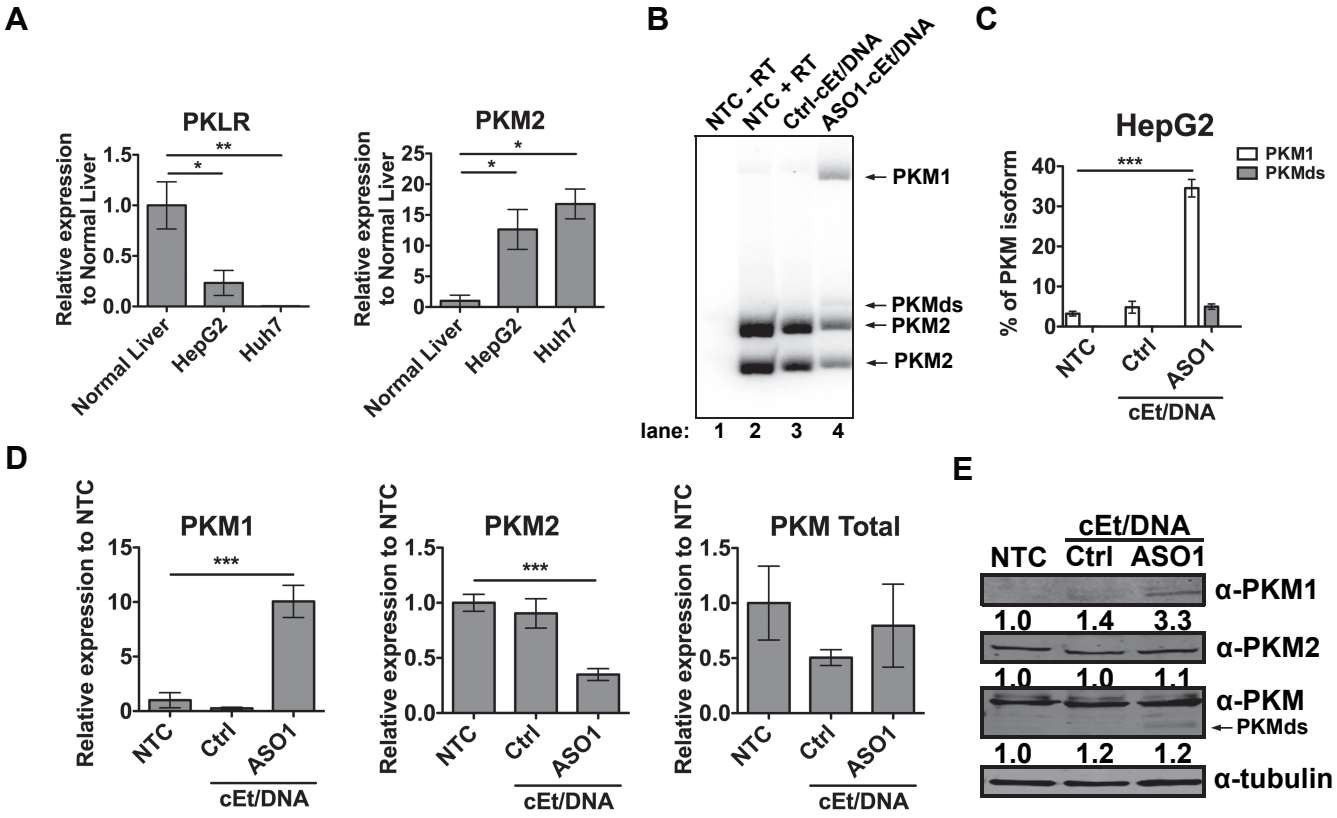

Supplementary Figure 1. PKM2 is the predominant isoform in HCC cells, and transfection of ASO1-cEt/DNA induces *PKM* splice switching in HepG2 cells

(A) RT-qPCR analysis of *PKLR* and *PKM2* transcript levels in different HCC cell lines and normal human liver. All tested transcripts were normalized to *HPRT* transcript level. Relative expression to normal liver is shown. (B) Radioactive RT-PCR analysis shows the degree of *PKM* splice switching after transfecting HepG2 cells with 60 nM ASO for two days. (C) Quantification of PKM1 and PKMds isoforms in panel (B). (D) RT-qPCR shows transcript levels after ASO treatment as in panel (B). All tested transcripts were normalized to *HPRT*, and relative expression to NTC is shown. (E) Western blotting analysis of PKM isoform switch. Protein lysates were prepared after ASO treatment as in panel (B), with quantification of band intensities shown below; bands were normalized to tubulin and to the NTC. The bar charts in panels (A, C, and D) represent the average of three independent biological replicates ± SEM. One-way ANOVA was performed with Dunnett's multiple comparison post-hoc test. * $P \leq 0.05$; ** $P \leq 0.01$; *** $P \leq 0.001$.

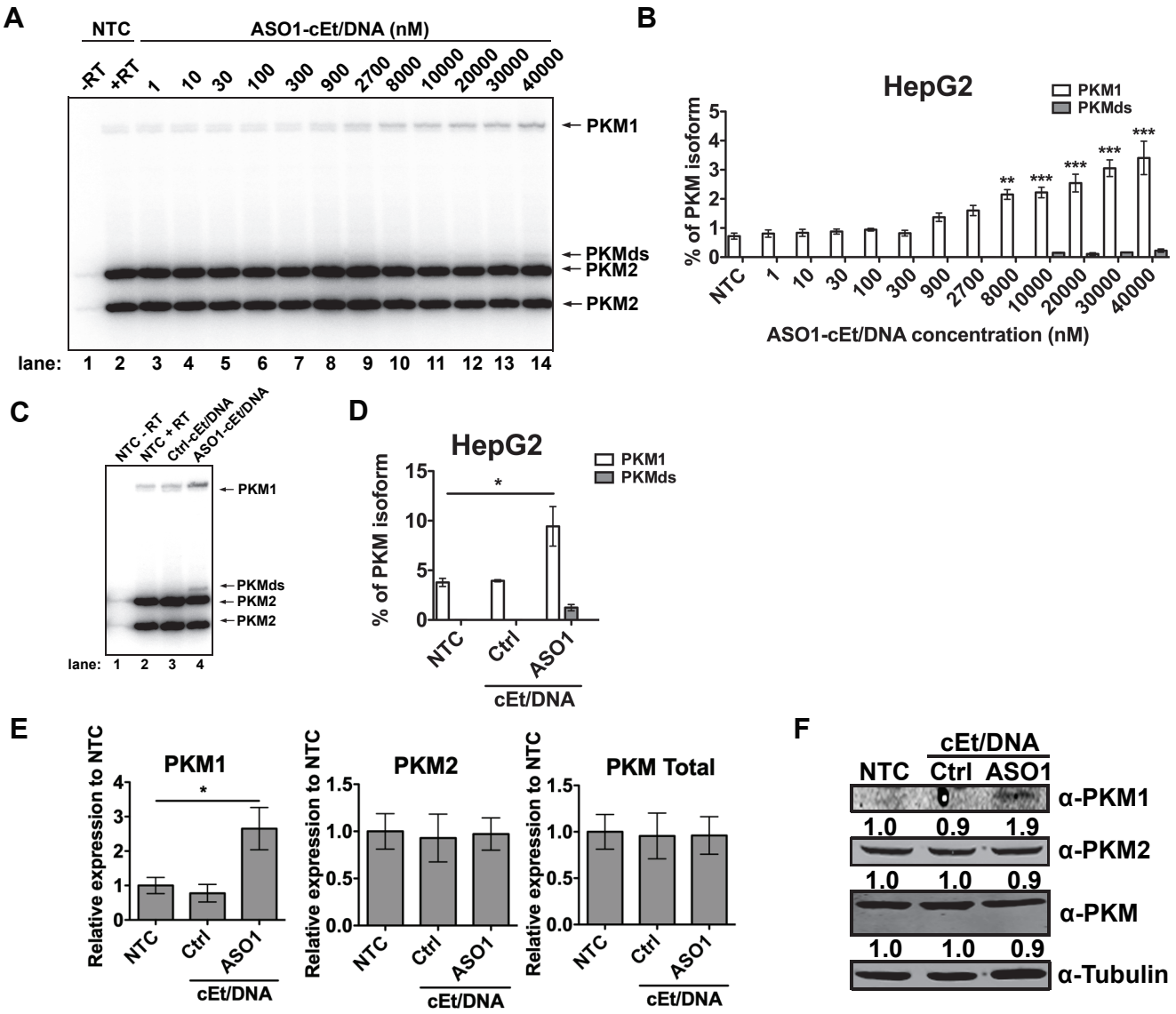

Supplementary Figure 2. Delivery of ASO1-cEt/DNA by free uptake induces *PKM* splice-switching in HepG2 cells

(A) ASO1-cEt/DNA induces *PKM* splice switching in a dose-dependent manner. Radioactive RT-PCR analysis of HepG2 cells treated with varying concentrations of ASO by free uptake for 4 days. (B) Quantification of PKM1 and PKMds isoforms in panel (A). (C) Radioactive RT-PCR analysis of RNA from HepG2 cells incubated with 20 μM ASO by free uptake for 7 days. Medium and ASO were replenished on day 4. (D) Quantification of PKM1 and PKMds isoforms in panel (C). (E) RT-qPCR quantitation of the indicated transcripts upon ASO treatment as in panel (C). All tested transcripts were normalized to the *HPRT* transcript level. Relative expression to the NTC is shown. (F) Western blotting analysis of PKM isoform switch, after treating HepG2 cells with 20 μM ASO as in panel (C), with quantification of band intensities shown below; bands were normalized to tubulin and to the NTC. The bar charts in panels (B, D, and E) represent the average of three independent biological replicates ± SEM. One-way ANOVA was performed with Dunnett's multiple comparison post-hoc test. * $P \leq 0.05$; ** $P \leq 0.01$; *** $P \leq 0.001$.

Supp. Figure 3

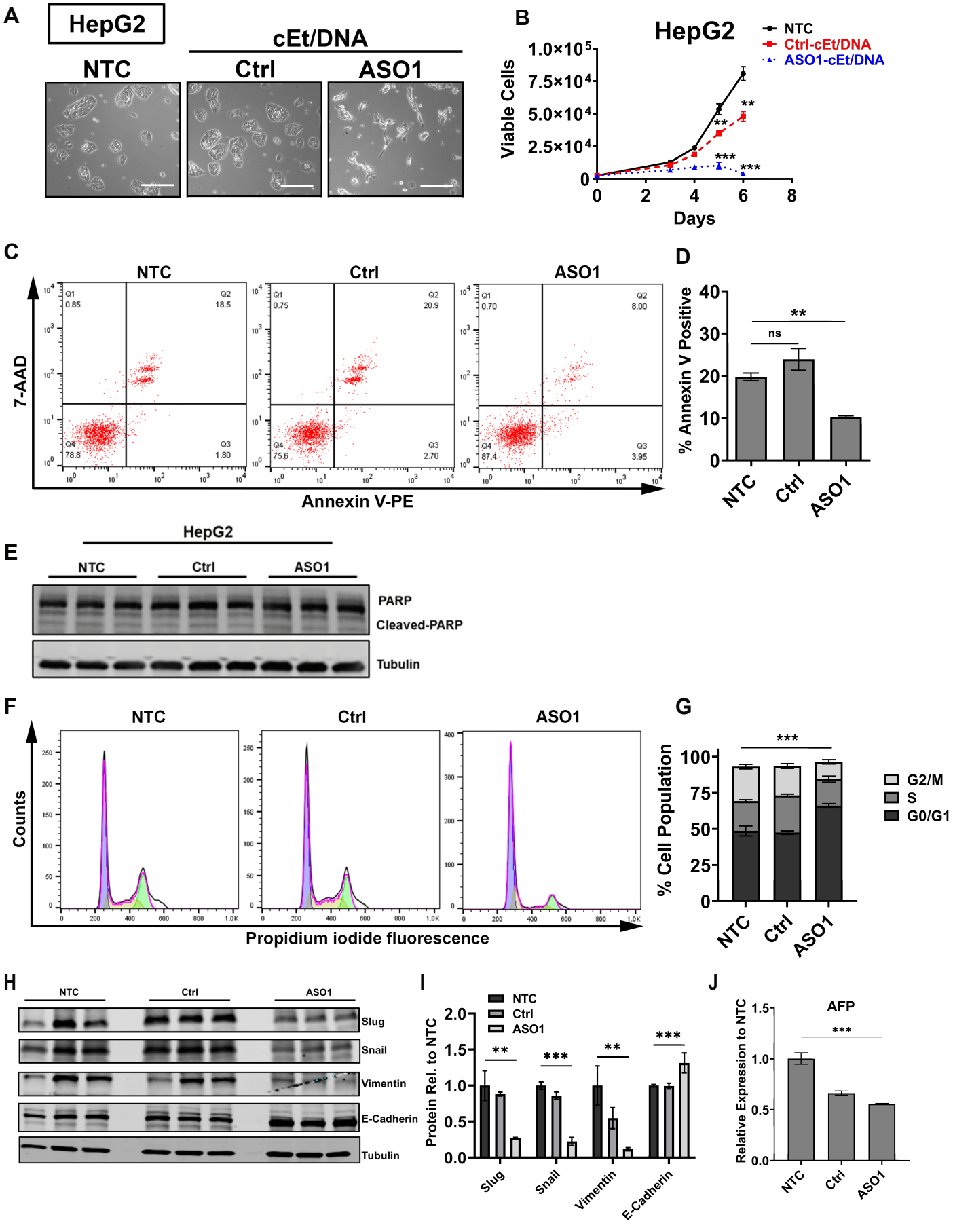

Supplementary Figure 3. ASO1-cEt/DNA inhibits HepG2 cell growth *in vitro*

(A) ASO1-cEt/DNA is toxic to HCC cells. Representative images of HepG2 cells following NTC, Ctrl-cEt/DNA, or ASO1-cEt/DNA treatment. Scale bar = 200 μm. (B) ASO1-cEt/DNA slows down growth of HepG2 cells. Viable cells were counted using ViaCount with flow cytometry. HepG2 cells were treated with 20 μM ASO by free uptake for the indicated time points. (C) Representative flow cytometry analysis of dual staining with Annexin V and 7-AAD in HepG2 cells treated with 20 μM ASO by free uptake for 5 days. (D) Quantification of Annexin V-positive cells in panel (C). (E) Western blot analysis of cleaved PARP in HepG2 cells treated as in panel (C). (F) Representative cell-cycle analysis of propidium iodide DNA staining in HepG2 cells treated with 20 μM ASO by free uptake for 6 days. (G) Quantification of cell-cycle analysis in panel (F); significance refers to the comparison between the G0/G1-population or the G2/M-population. Differences in the S-population were not significant. (H) Western blot analysis of molecular markers of EMT in HepG2 cells treated as in panel (F). (I) Quantification of Western blot analysis from panel (H). (J) RT-qPCR quantitation of alpha-fetoprotein (AFP) in HepG2 cells treated with ASO1-cEt/DNA for 7 days. All tested transcripts were normalized to the *HPRT* transcript level. Relative expression versus the NTC is shown. All data in panels (B-J) represent the average of three independent biological replicates ± SEM. One-way ANOVA was performed with Dunnett's multiple comparison post-hoc test. * $P \leq 0.05$; ** $P \leq 0.01$; *** $P \leq 0.001$.

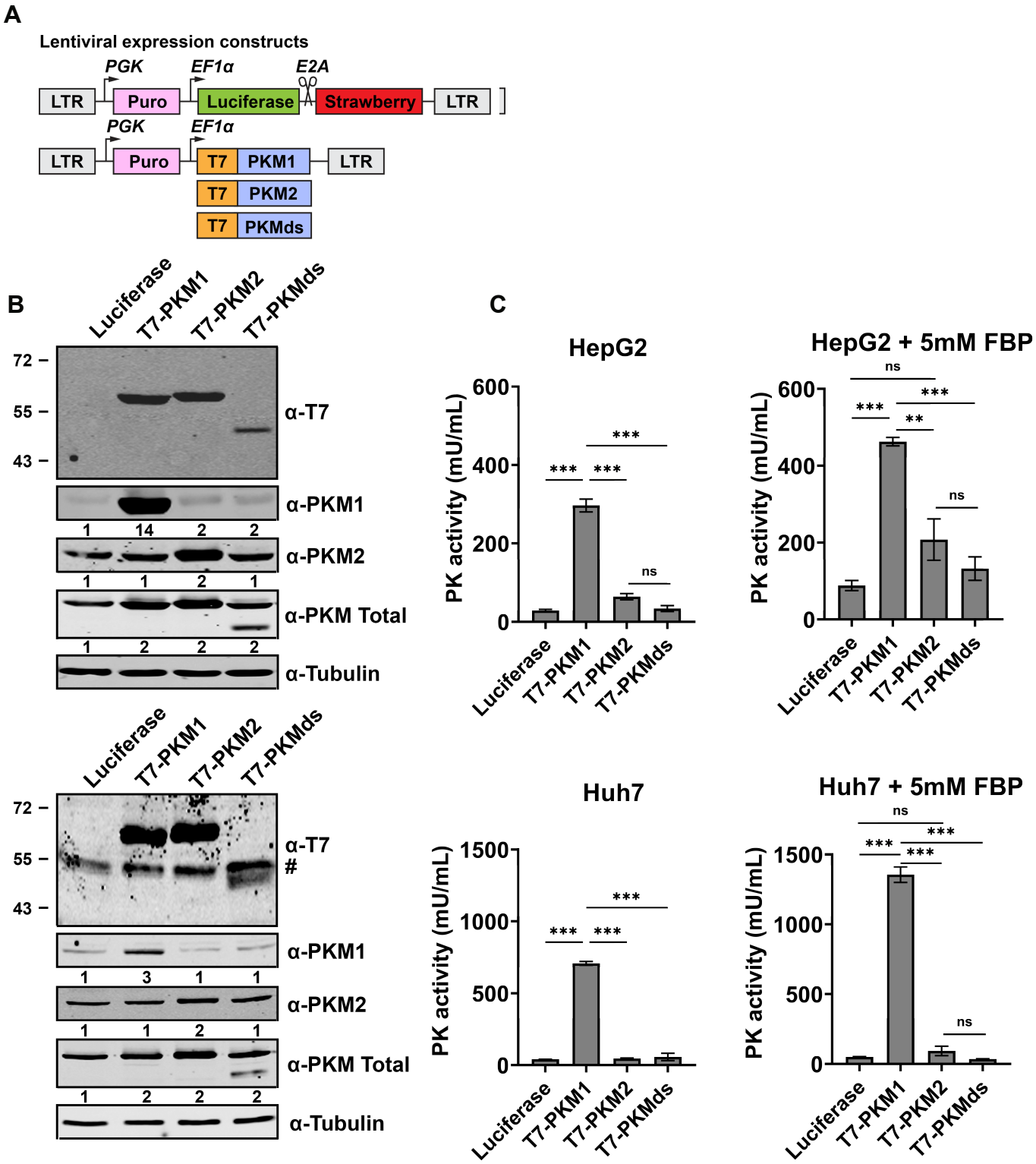
A
Lentiviral expression constructs
PGK
EF1α
E2A
LTR
Puro
Luciferase
Strawberry
LTR
PGK
EF1α
LTR
Puro
T7
PKM1
LTR
T7
PKM2
T7
PKMds
B
Luciferase
T7-PKM1
T7-PKM2
T7-PKMds
72
55
43
α-T7
α-PKM1
1 14 2 2
α-PKM2
1 1 2 1
α-PKM Total
1 2 2 2
α-Tubulin
Luciferase
T7-PKM1
T7-PKM2
T7-PKMds
72
55
43
α-T7
#
α-PKM1
1 3 1 1
α-PKM2
1 1 2 1
α-PKM Total
1 2 2 2
α-Tubulin
C
HepG2
PK activity (mU/mL)
600
400
200
0
***
***
***
ns
Luciferase
T7-PKM1
T7-PKM2
T7-PKMds
HepG2 + 5mM FBP
PK activity (mU/mL)
600
400
200
0
ns
***
***
**
ns
Luciferase
T7-PKM1
T7-PKM2
T7-PKMds
Huh7
PK activity (mU/mL)
1500
1000
500
0
***
***
***
Luciferase
T7-PKM1
T7-PKM2
T7-PKMds
Huh7 + 5mM FBP
PK activity (mU/mL)
1500
1000
500
0
ns
***
***
***
ns
Luciferase
T7-PKM1
T7-PKM2
T7-PKMds

Supplementary Figure 4. Enforced expression of individual PKM isoforms

(A) Schematic diagram of different T7-tag PKM isoforms and luciferase-strawberry cDNAs that were individually cloned into a lentiviral expression vector, which carries a puromycin-selection marker. (B) Various T7-tag PKM isoforms were successfully expressed in HepG2 (top) and Huh7 (bottom) cells, as detected by Western blotting. Numbers below the blots indicate the fold change relative to cells expressing luciferase-strawberry; # indicates a non-specific band. (C) T7-PKM1 and T7-PKM2 isoforms are catalytically active. Pyruvate kinase assays were performed in cell lysates incubated with or without 5 mM FBP for 30 min at room temperature. Data shown are from the 10-min timepoint. Pyruvate kinase activity was normalized to 5×10^4 cells. All data in panel (C) represent the average of three independent biological replicates ± SEM, except for T7-PKM2 and T7-PKMds in Huh7 with FBP (N=2). One-way ANOVA was performed with Tukey's multiple comparison post-hoc test. * $P \leq 0.05$; ** $P \leq 0.01$; *** $P \leq 0.001$.

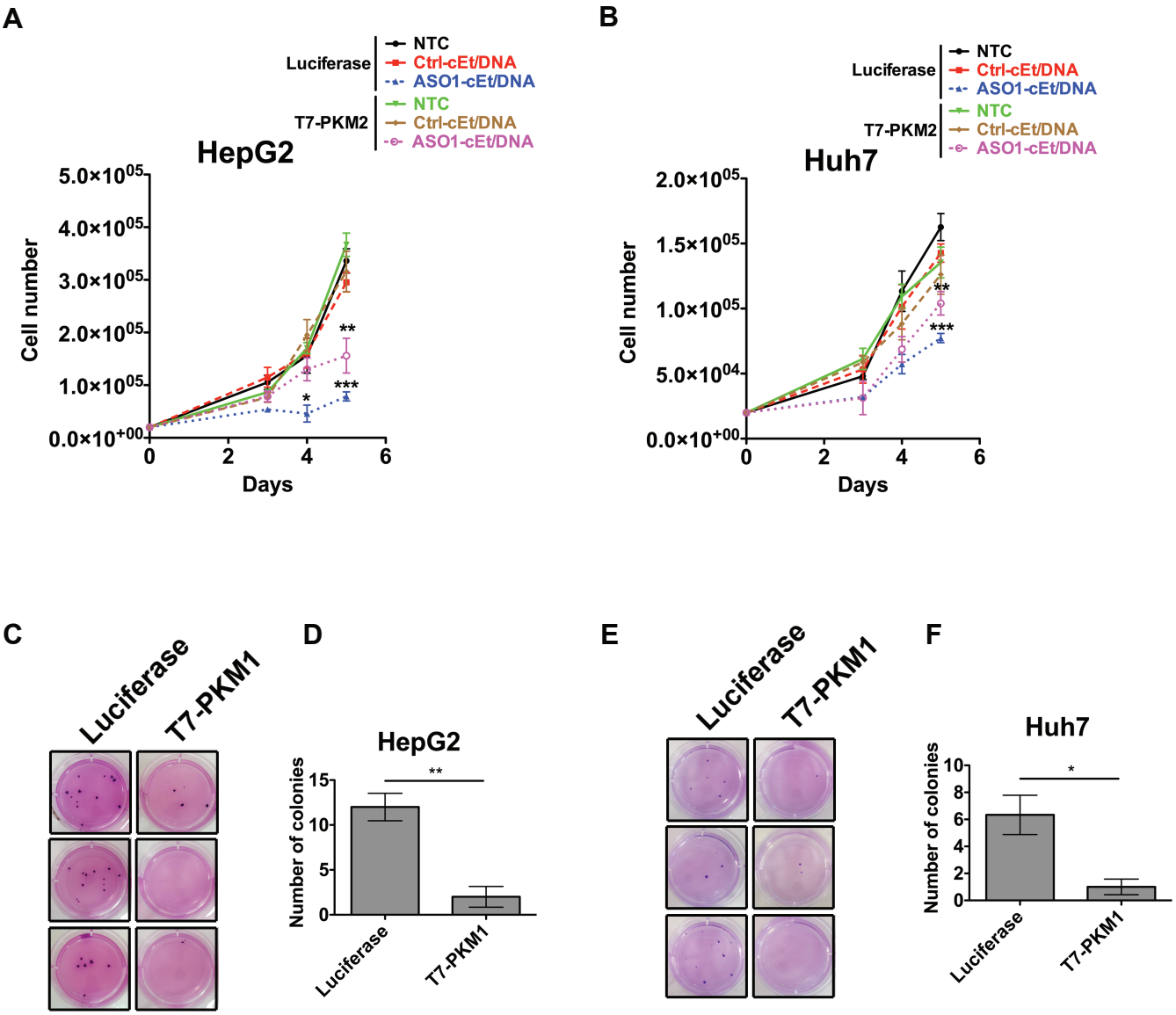

Supplementary Figure 5. ASO1-cEt/DNA-dependent slow-growth phenotype is an on-target effect, and enforced expression of PKM1 is sufficient to inhibit HCC cell growth

(A - B) Enforced expression of PKM2 partially rescues the ASO1-cEt/DNA-dependent slow-growth phenotype. Cells were counted with a hemocytometer. HepG2 and Huh7 cells expressing T7-PKM2 or luciferase-strawberry were treated with 20 μM ASO by free uptake for the indicated times. (C) Soft-agar assay was performed in HepG2 cells expressing luciferase-strawberry or T7-PKM1. 10,000 HepG2 cells/well were plated with soft agar and incubated at 37 °C/5% CO_2 for 2 months. (D) Quantification of the number of colonies in panel (C). (E) Soft-agar assay with Huh7 cells expressing luciferase-strawberry or T7-PKM1. 50,000 Huh7 cells/well were plated with soft agar and incubated at 37 °C/5% CO_2 for 3 weeks. (F) Quantification of the number of colonies in panel (E). All data in panels (A, B, D, and F)) represent the average of three independent biological replicates ± SEM. One-way ANOVA was performed with Dunnett's multiple comparison post-hoc test. * $P \leq 0.05$; ** $P \leq 0.01$; *** $P \leq 0.001$.

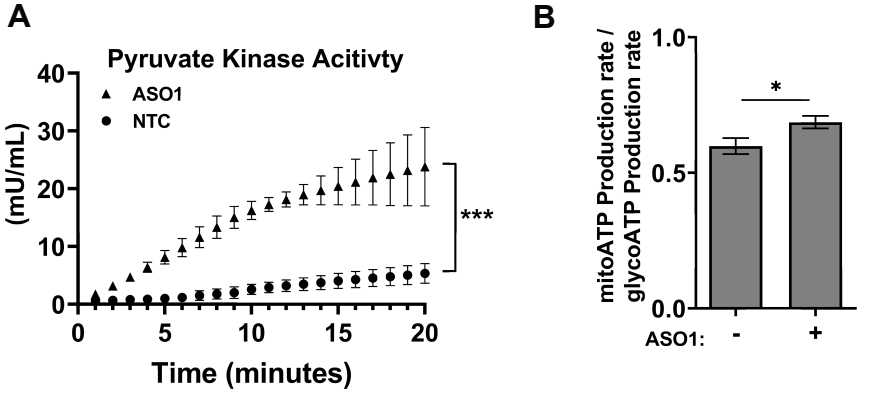

Supplementary Figure 6. ASO1-cEt/DNA increases pyruvate kinase activity and mitochondrial ATP production rate in HepG2 cells

(A) Pyruvate kinase activity in HepG2 cells increased upon ASO1-cEt/DNA treatment. Pyruvate kinase assay was performed after treating HepG2 cells with 20 μM ASO by free uptake for four days. Pyruvate kinase (PK) activity was normalized to 5×10^4 cells. The graph represents the average of three independent biological replicates ± SEM. (B) ASO1-cEt/DNA increases mitochondrial ATP production rate. Seahorse extracellular flux analysis showing the ratio of mitochondrial ATP production rate (mitoATP) to glycolytic ATP production rate (glycoATP) in HepG2 cells treated with 20 μM ASO by free uptake for 7 days. Medium and ASO were replenished on day 4. Production rate refers to pmol ATP/min/10^3 cells. Data are the average of 6independent cultures ± SEM. One-way ANOVA was performed with Dunnett's multiple comparison post-hoc test in panel (A). A linear mixed-effects model was used to determine significance in panel (B). * $P \leq 0.05$; ** $P \leq 0.01$; *** $P \leq 0.001$.

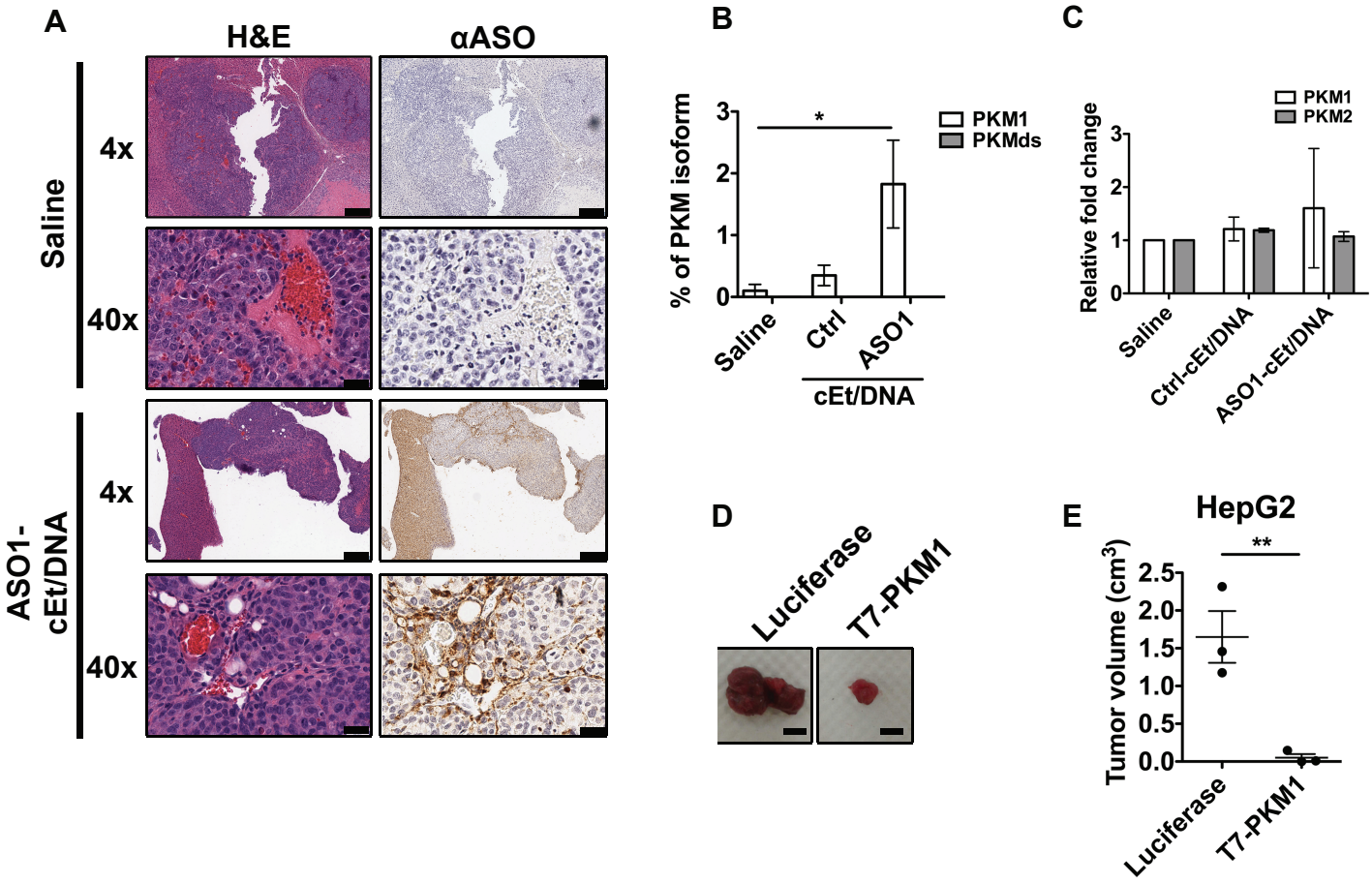

Supplementary Figure 7. ASO1-cEt/DNA is taken up by HCC tumors in the xenograft model, and enforced expression of PKM1 is sufficient to inhibit HCC cell growth *in vivo*

(A) Representative pictures of immunohistochemistry analysis of ASO localization in liver sections with tumors on day 29. Rabbit anti-ASO antibody recognizes the phosphorothioate backbone. H&E staining of the corresponding sections is shown. Scale bar = 250 μm for 4× and 25 μm for 40×. (B) ASO1-cEt/DNA induces *PKM* splice switching in a HepG2 xenograft model. Radioactive RT-PCR was performed on liver-tumor samples removed from the transplanted mice on day 29. Quantification of PKM1 and PKMds isoforms is shown. (C) Western blotting analysis of PKM isoform switch in HepG2 xenografts. Protein lysates were extracted from liver-tumor samples removed from the transplanted mice on day 29. Quantification of PKM1 and PKM2 isoforms is shown. (D) Enforced expression of PKM1 is sufficient to inhibit HepG2 cell growth *in vivo*. Representative pictures of tumors on day 29. Scale bar = 5 mm. (E) Quantification of tumor volume in panel (D). All data in panels (B, C, and E) are the average of three biological replicates ± SEM. One-way ANOVA was performed with Dunnett's multiple comparison post-hoc test. * $P \leq 0.05$; ** $P \leq 0.01$; *** $P \leq 0.001$.

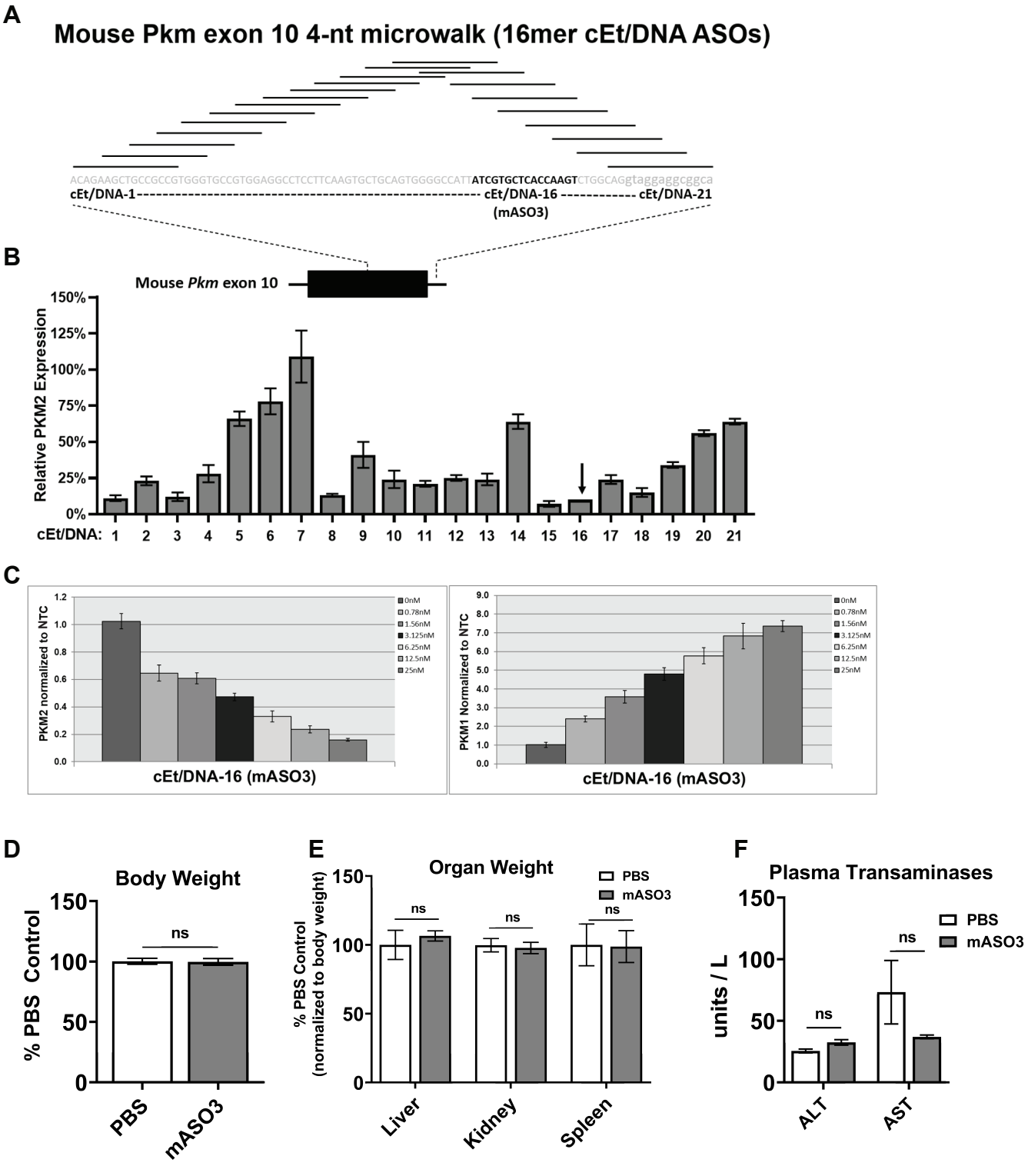
A
Mouse Pkm exon 10 4-nt microwalk (16mer cEt/DNA ASOs)
ACAGAAGCTGCCGCCGTGGGTGCCGTGGAGGCCTCCTTCAAGTGCTGCAGTGGGGCCATTATCGTGCTCACCAAGTCTGGCAGgtaggaggcggca
cEt/DNA-1
cEt/DNA-16
cEt/DNA-21
(mASO3)
B
Mouse Pkm exon 10
Relative PKM2 Expression
150%
125%
100%
75%
50%
25%
0%
cEt/DNA: 1 2 3 4 5 6 7 8 9 10 11 12 13 14 15 16 17 18 19 20 21
C
PKM2 normalized to NTC
0nM
0.78nM
1.56nM
3.125nM
6.25nM
12.5nM
25nM
cEt/DNA-16 (mASO3)
PKM1 Normalized to NTC
cEt/DNA-16 (mASO3)
D
Body Weight
% PBS Control
ns
PBS
mASO3
E
Organ Weight
% PBS Control (normalized to body weight)
PBS
mASO3
ns
Liver
Kidney
Spleen
F
Plasma Transaminases
units / L
PBS
mASO3
ns
ALT
AST

Supplementary Figure 8. Screening approach to identify mASO3-cET/DNA, and analysis of systemic toxicity in mASO3-cEt/DNA-treated C57BL6 mice

(A) Schematic of 16mer ASO 4-nt microwalk along *mPKM* exon 10 (upper case), and part of intron 10 (lower case). Each 16mer ASO has mixed cEt/DNA chemistry. The lead mASO #16 (mASO3-cEt/DNA) and the region of *mPKM* exon 10 to which it binds is highlighted in bold. (B) RT-qPCR of *mPKM2* expression in the MHT murine hepatocellular SV40 large T-antigen carcinoma cell line transfected with 50 nM ASO for 24 h using ASOs from panel (A). Transcripts were normalized to total RNA (RiboGreen), and compared to no-treatment control cells (NTC). Arrow indicates mASO #16 (mASO3-cEt/DNA). (C) Representative RT-qPCR of *mPKM1* and *mPKM2* expression in bEND murine endothelial cells transfected with varying concentrations of ASO (mASO3-cET/DNA) for 24 h. Transcripts were normalized to total RNA (RiboGreen), and compared to NTC. (D) Representative body weight and (E) organ weights of C57BL6 mice treated with PBS or ASO (mASO3-cET/DNA) at 100 mg/kg/wk. (F) Representative ALT and AST levels in serum collected from mice 48 h after the last dose. All data in panels (D - F) are the average of 4 male mice per group, using two-tailed unpaired t-test with ± SEM shown. * $P \leq 0.05$; ** $P \leq 0.01$; *** $P \leq 0.001$.

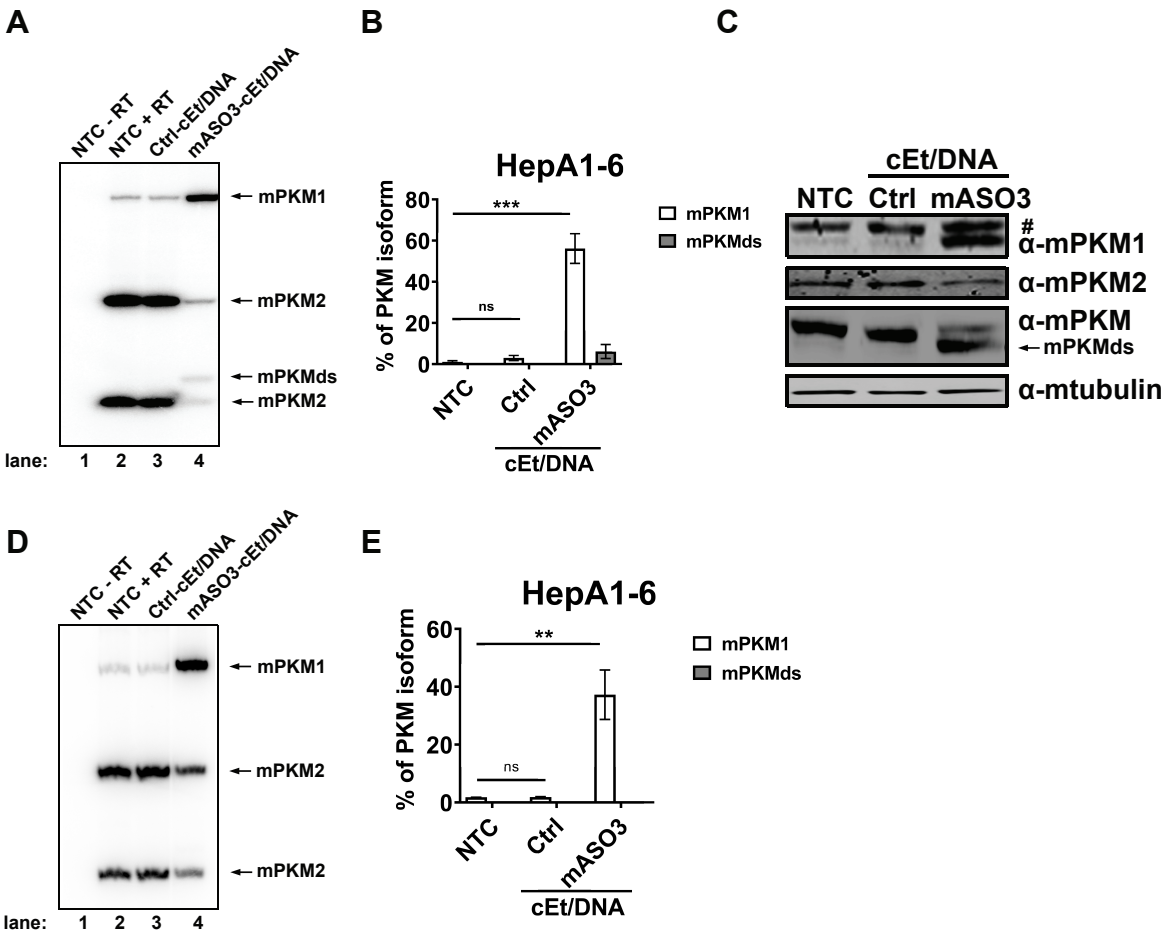

Supplementary Figure 9. mASO3-cEt/DNA induces *mPKM* splice-switching in HepA1-6 cells

(A) Radioactive RT-PCR analysis of HepA1-6 murine hepatoma cells transfected with 60 nM mASO3-cEt/DNA. (B) Quantification of PKM1 and PKMds isoforms in panel (A). (C) Western blotting analysis of mPKM isoforms. # indicates a non-specific band. (D) Radioactive RT-PCR analysis of HepA1-6 cells treated with 20 μM mASO3-cEt/DNA by free uptake for 7 days. The medium and ASO were replenished on day 4. (E) Quantification of PKM1 and PKMds isoforms in panel (D). All data in panels (B and E) are the average of three biological replicates ± SEM. One-way ANOVA was performed with Dunnett's multiple comparison post-hoc test. * $P \leq 0.05$; ** $P \leq 0.01$; *** $P \leq 0.001$.

Supp. Figure 10

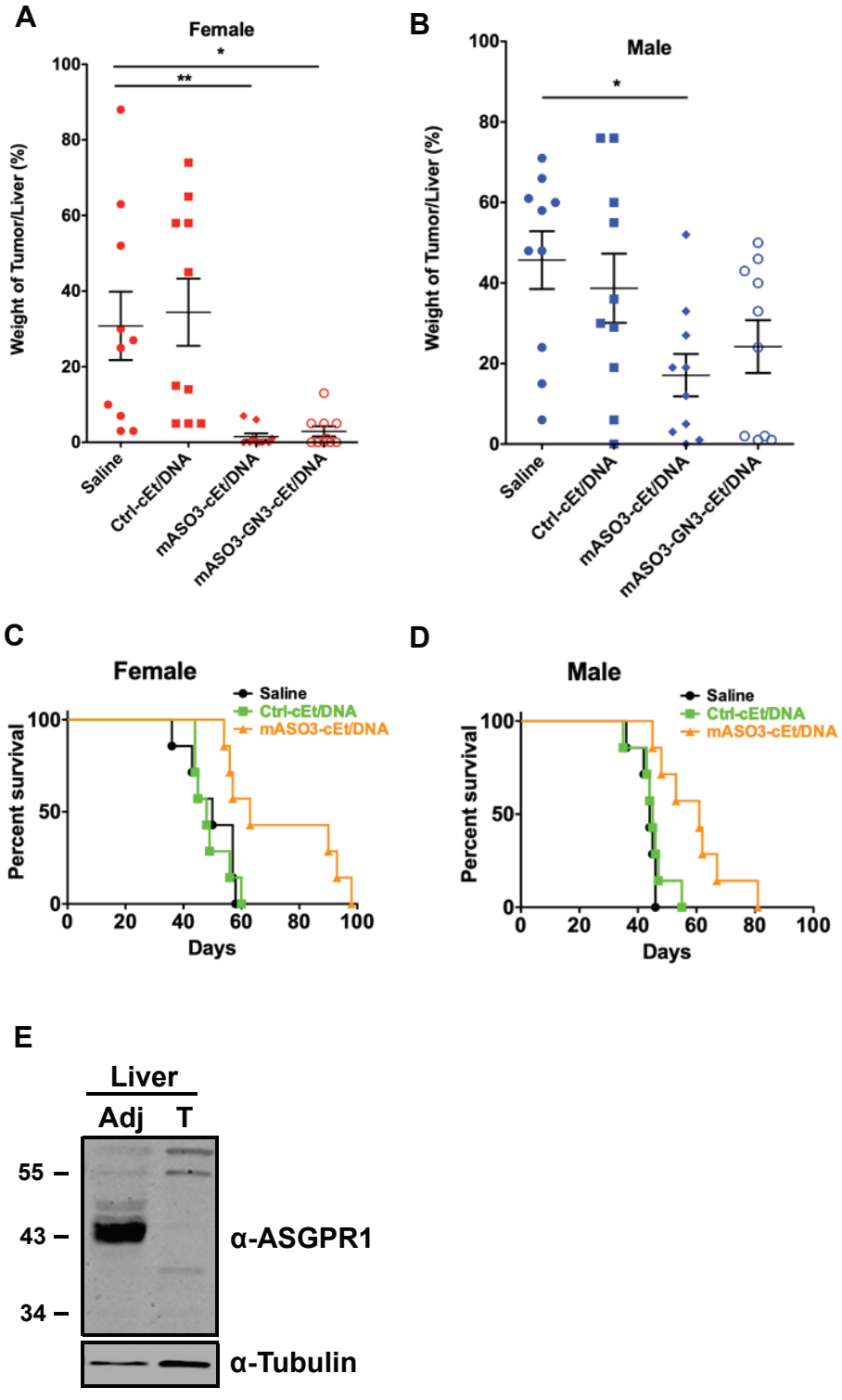

Supplementary Figure 10. Sexual dimorphism in HCC mice treated with mASO3-cEt/DNA, and absence of ASGPR1 in mouse HCC

(A, B) Measurements of tumor weight normalized to the weight of the whole liver in (A) male mice and (B) female mice in different treatment groups on day 47. A total of 40 mice (N = 10 per group) were randomized to each treatment group. (C, D) Survival analysis in (C) male and (D) female mice. A total of 21 mice (N = 7 per group) were randomized in each treatment group. Log-rank test with Bonferroni-corrected threshold (P = 0.0166) was separately done for male and female mice. For male mice, saline-treated mice had a median survival of 44 days; Ctrl-treated mice had a median survival of 45 days (P = 0.3441); and mASO3-treated mice had a median survival of 61 days (P = 0.0013). For female mice, saline-treated mice had a median survival of 50 days; Ctrl-treated mice had a median survival of 48 days (P = 0.9371); and mASO3-treated mice had a median survival of 63 days (P = 0.0217). (E) ASGPR1 is down-regulated in a liver tumor. Western blotting analysis of protein lysate from a liver tumor (T) or the adjacent normal 6B (Adj) on Day 47.